Large Scale Wavelength Routing Optical Switch for Data Center Networks

Ken-ichi Sato, Hiroshi Hasegawa, Tomonobu Niwa, Nagoya University
Toshio Watanabe, NTT Photonics Laboratories

ABSTRACT---Intra data center traffic is estimated to be about four times the global Internet traffic and is continuously increasing. Applying optical switching to datacenter networks will increase network bandwidth and reduce power consumption while meeting the traffic requirements. One of the major attributes of the optical switch must be scalability. The wavelength routing switch is a promising technology for the development of 1,000x1,000 scale large port count optical switches. Recent advances are demonstrated.

INTRODUCTION

Intra data center traffic is estimated to be about four times the global Internet traffic and the CAGR is about 30 % [1]. In a data center, traffic flow is changing from North-South to East-West, that is between servers/storages within a data center rather than inbound/outbound traffic. It is impressive to note that, for example, a single 1 kB HTTP request generates 930 kB of internal network traffic [2]. Reflecting the traffic increase and the needs for simplifying networks and cabling, and for enhanced scalability and flexibility, reduced tier network architectures that utilize giant throughput electrical switches are recently being considered [3]. The reduced tier architecture minimizes oversubscription of switch capacities and reduces the latency caused by the lack of network capacity. The front surface of the electrical switches tends to be fully covered with transceiver modules and the power consumption limits the density. The increase in processing and communication capacities required in data centers has also caused a tremendous increase in the power consumption of electrical switches and routers. To fundamentally resolve the power consumption and transponder cost issues of large electrical switches, the off-loading of large traffic flows from the electrical layer to the optical layer is expected to play a key role. In this context, new data center network architectures that exploit optical switching technologies are now being explored. Leveraging optical fast circuit switching alongside electrical packet switching is recognized to be one of the most attractive solutions [4-9]. With the hybrid network solution, optical circuit switching offers the ability needed to economically reconfigure networks to support giant data flows with low latency and can scale as needed to 40 or 100 GB/s or even beyond without scaling hardware size or electrical power consumption. In the network, the giant data flows between specific top-of-rack switches (ToRs) or pods will be delivered by optical circuit switches [4-9]. In a large datacenter, a server rack with ToR switch is considered as a single endpoint system rather than a datacenter network. The effectiveness of this approach will be enhanced as the ratio of giant data flows (it is well known that in datacenters a small number of large flows dominates total traffic volume) and interface speeds increase. However, clear requirements for optical circuit switches in datacenters or the breakeven points against electrical switching have yet to be identified. Although the maturity level of today's optical switching technology currently prevents this, it is conceived that 100-300 ports will be inadequate and switching time of 10-100 μs will be transformative for effectively offloading traffic from electrical Ethernet switches [10].

To implement optical circuit switching, the various technologies being considered include; high port count MEMS switches [4,5], wavelength selective switches (WSS) [6], combinations of wavelength tunable lasers and arrayed waveguide gratings (AWGs) [7][8], and semiconductor optical amplifier (SOA) based switches [9]. The major parameters used to determine approach effectiveness are switch scalability and switching speed [10], to say nothing of cost. The target switching time can be sub-microsecond [7] with switch size of 1,000x1,000. 3D MEMS switches have relatively slow switching times, the order of a few milliseconds. The switching time of the LCoS based WSS is usually more than 100 ms. The SOA based approach will attain the target speed, but the power consumption and optical signal to noise ratio of the cascaded SOA gates severely limit the available scale. At present, a 16x16 SOA based switch that has been fabricated on a single chip integrates more than one thousand functional components [9].

The wavelength routing approach that combines wavelength tunable lasers and arrayed waveguide grating routers (AWGRs) exhibits some unique advantages. The switching speed is determined by the laser wavelength tunability, and tuning speeds can be less than 100 nanoseconds. Wavelength routing is a built-in function of the passive AWGR and it does not needs any optical path alignment manipulation at the manufacturing stage; space division switches such as 3D MEMS on the other hand requires 10^6

manipulations to set 1,000x1,000 optical paths at the initial mirror setting stage. However, the major barrier is the scalability needed to reach the 1,000 port count. This article discusses breakthrough technologies and demonstrates recent advances.

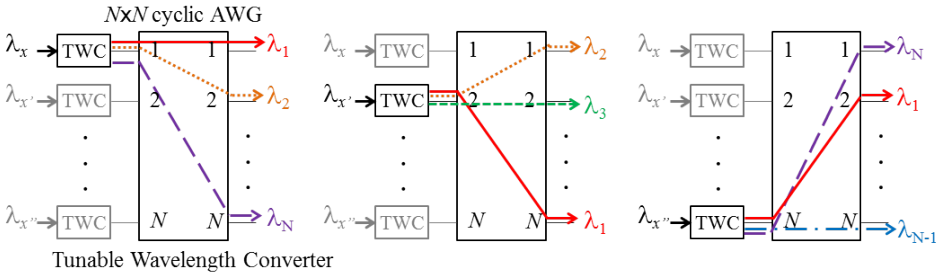

Fig. 1. Wavelength routing of a cyclic AWG for different input ports

WAVELENGTH ROUTING SWITCH

Wavelength Routing (WR)-switches are capable of switching input signals to arbitrary output ports by changing the laser wavelength at each input port. When the input signal is optical, a tunable wavelength converter (TWC), which can be a compact tunable transceiver (for example, a type of commercially available tunable multirate XFP transceiver), will be applied. A basic *N*x*N* WR-switch that routes *N* equally spaced wavelengths λ_1, ..., λ_N is shown in Fig. 1. It consists of *N* TWCs and a single *N*x*N* cyclic AWG whose free spectral range (FSR) is *N* times the channel frequency spacing. In the cyclic AWG, the relation among the input port number (*# input port*), the output port number (*# output port*), and wavelength index number (*# wavelength*) is given by

$$\#\ output\ port = (\#\ wavelength - \#\ input\ port)_{mod\ N} + 1 \qquad (1)$$

The input/output ports of the cyclic AWG are efficiently utilized. The WR-switch utilizing a single *N*x*N* cyclic AWG offers a simple architecture for wavelength routing and this architecture achieves non-blocking *N*x*N* switching. However, there are two major barriers to attaining large port count cyclic AWGs. One is the deviation of passband center frequencies from the ITU-T grid. It becomes very large as *N* becomes large [11], so the number of input/output ports, *N*, is limited in practice. For example, with a 32x32 AWG for 32 channels with 100 GHz spacing, the worst frequency deviation value is 44.5 GHz. One possible approach to mitigating the effect of AWG frequency deviation is to tune the wavelengths of each TWC to the center of each passband of the AWG, however, controlling tunable lasers becomes complicated (present commercially available tunable transceivers use a simple frequency locker to conform to the ITU-T grid). Good performance and cost-effectiveness can be attained by developing a large-scale WR-switch using small AWGs with small passband deviation.

Another major issue to be resolved is the cross-talk that increases with the port count increase [8]. In order to realize large scale optical switches, one viable solution is to bridge several wavelength routing parts by optical switches. For example, a 448 x 448 OXC prototype was demonstrated [8] where 100 GHz spaced cyclic 32 x 32 AWGs are bridged by DC (delivery and coupling)-switches [12] and WDM couplers. More than 64 100GHz spaced wavelengths are used for routing, which imposes the costly requirement of wide-range laser tunability. OXC port count can be effectively enlarged by increasing the port count of the cyclic AWGs. The ULCF (uniform-loss and cyclic-frequency) configuration has been developed; [11] shows a prototype 64x64 AWG router that utilizes a 64x128 AWG and 64 1x2 couplers, where each pair of AWG output ports are bridged as one router output so that the passband deviation is reduced. However, the port count is still too small to support the envisaged applications; increasing the port number requires a larger port count component AWG and more couplers, which seems to be impractical.

In order to resolve the above mentioned problems with realizing large scale AWG routers, a novel architecture that cascades small cyclic AWGs of different sizes has recently been proposed [13]. The architecture exhibits the salient features of; 1) ITU-T specified fixed grid frequencies are utilized (a

version of commercially available cost effective transceivers can be utilized), 2) the use of small cyclic AWGs offers smaller total cross-talk level, 3) high scalability sufficient to reach 1,000 ports, and 4) good modular growth capability. So far, the wavelength routing capability of a 90 x 90 50GHz-spaced wavelength routing system prototype that consists of discrete components has been experimentally confirmed [13], and a 270 x 270 optical switch that consists of ninety 3 x 3 DC-switches [12] and three 90 x 90 proposed AWG subsystems, all of which are mounted in a 370 x 230 x 120 mm^3 box has been demonstrated and optical performance was confirmed by transmission experiments [14]. The details are presented below.

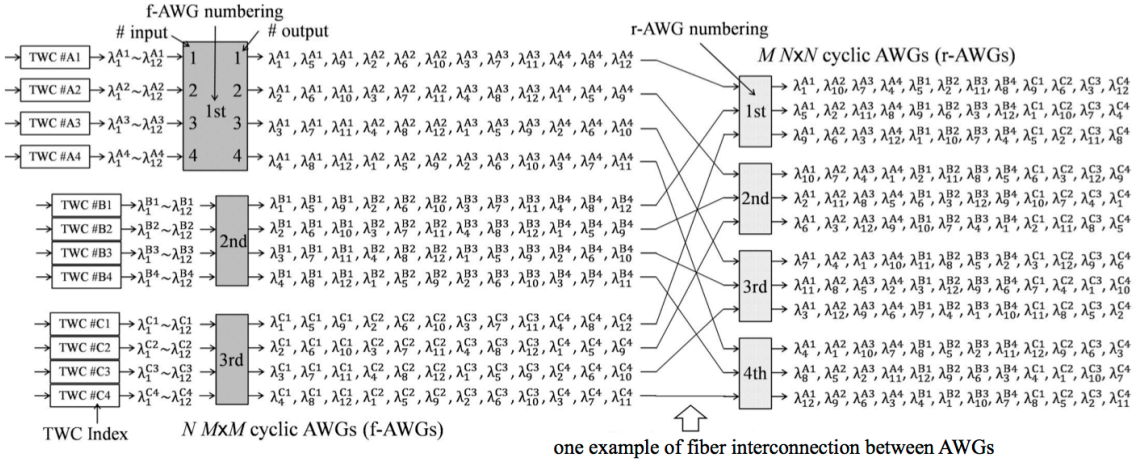

Fig. 2 Novel wavelength routing switch architecture (MNxMN subsystem) and the wavelength map (M = 4 and N = 3)

WAVELENGTH ROUTING SWITCH EMPLOYING CYCLIC AWG INTERCONNECTION

Fig. 2 shows the novel wavelength routing switch configuration that combines small AWGs of different sizes. In this configuration, *N* *M*x*M* cyclic AWGs (front(f)-AWGs) and *M* *N*x*N* cyclic AWG (rear(r)-AWGs) are connected so that each f-AWG is connected to all r-AWGs by single fibers, where an example for the case of $M = 4$ and $N = 3$ is shown for simplicity. The AWG input port index (#input), output port index (#output), f-AWG and r-AWG numbering, and TWC indices (#A1, #A2, ..., #C4) are given in Fig. 2. The figure explains how the AWG output port index is changed according to the input wavelength variation. Each TWC can select any wavelength from λ_1 to λ_{12}, and hence any output port can be selected by assigning an appropriate wavelength at TWC. Wavelength indices of the output wavelengths from each f-AWG output port (e.g. λ_1, λ_{1+M}, λ_{1+2M}, ...) appear cyclically with *M* spacing, and these wavelengths need to be delivered to different output ports in the next stage AWGs. Hence the degrees of AWG port count, *M* and *N*, must differ from each other. The port counts of the f-AWGs and r-AWGs are determined by considering the following restriction; *M* and *N* (≥2) must be mutually co-prime numbers [20] so that any input port can be connected to any output port with a specific wavelength. For example, $(M, N) = (N+1, N)$ fulfills this requirement. This configuration has the same wavelength routing capability as a single *MN*x*MN* AWG. If *M* and *N* are not co-prime, for example their greatest common divisor is 2, only half of the output ports can be used. Various connection patterns are possible between f-AWG output ports and r-AWG input ports. Let *i* (=1, 2, ..., *N*) be the index of f-AWG and *j* (=1, 2, ..., *M*) that of r-AWG. Let $\#f^i_{in}$, $\#f^i_{out}$ (=1, 2, ..., *M*) and $\#r^j_{in}$, $\#r^j_{out}$ (=1, 2, ..., *N*) be, respectively, the indexes of input/output ports of the *i*th f-AWG and *j*th r-AWG. In Fig. 2, we assume that the *i*th f-AWG is connected to the *j*th r-AWG so that $\#f^i_{out} = j$ and $\#r^j_{in} = i$; this is one example of the fiber interconnections possible.

There are several advantages to this architecture over the conventional approach that suit single large scale AWGs. A large port count routing device can be obtained by choosing large N and M values. The deviations from the ITU-T grid are suppressed due to the adoption of small-size component AWGs, which avoids the special arrangement needed in [11], and the port count can be much larger than that in

[11]. This configuration provides modular growth capability in terms of TWCs and f/r-AWGs. For example, suppose that an LxL ($L<MN$) switch is necessary in the initial installation. For this we connect $\lceil L/M \rceil$ MxM AWGs and $\lceil L/N \rceil$ NxN AWGs, where $\lceil \cdot \rceil$ represents the ceiling operation. This switch can be gradually expanded up to MNxMN by adding MxM and NxN AWGs. To enable this in a simple manner, interconnecting fibers among separate modules should be installed from the outset. The major cost of the system comes from optical device modules and not from interconnect fibers and multi-fiber connectors.

Table 1 Examples of switch scale

switch size in Fig. 2	M	N	# of necessary wavelenths
210x210	14	15	210
208x208	13	16	208
195x195	13	15	195
182x182	13	14	182
156x156	12	13	156
154x154	11	14	154
143x143	11	13	143
132x132	11	12	132
130x130	10	13	130
110x110	10	11	110
99x99	9	11	99
90x90	9	10	90
88x88	8	11	88
72x72	8	9	72
70x70	7	10	70

Table 1 shows examples of combinations of switch scale and parameters, M and N. In theory, this configuration can achieve a very large-scale wavelength routing function, for example, 210x210 in the case of M = 14, N = 15, but overall system optimization is important. The tunable frequency range of TWC limits the size of the proposed switch; an MNxMN wavelength routing switch requires a TWC tuning range of MN x (channel spacing) for switching. Commercially available tunable transceivers cover the entire C-band, realizing $MN \cong 90$ for 50 GHz grid spacing. This problem can be resolved by bridging multiple wavelength switches, for example, by using KxK delivery-coupling type switches [12].

In the proposed configuration, the basic requirement for interconnection is that each pair of f/r AWGs is bridged by an independent fiber. In other words, there is room for optimizing the selection of output/input ports of the AWGs (the interconnection pattern shown in Fig. 2 is but one example). The objective of optimization is to minimize the worst loss, which can be achieved by configuring the connection so that f/r AWGs will not yield large loss simultaneously. However, the number of possible connections is extremely large (the number of possible combinations is $(M!)^N$x$(N!)^M$) and hence it is hard to find the truly optimal connection. A method to find suboptimal solutions by local search has been developed. Each f/r AWG has almost the same transmission loss characteristics; loss between center input/output ports is generally small while that between edge ports is large. For each pair of f/r-AWGs, we specify the input port number of r-AWG for the interconnecting fiber as follows;

$$\#r_{in}^{j} = (i+j-2)_{mod\,N} + 1 \qquad (2)$$

where i and j are the respective indexes of the f/r-AWGs. For each f-AWG, input port indexes of the r-AWGs that are as different as possible are assigned so as to minimize the slant among f/r-AWG pairs. Next, the worst loss is minimized by checking all possible assignments of output ports of the f-AWGs. The number of possible assignments in each f-AWG is $M!$ and hence the computation time of this search is substantially reduced.

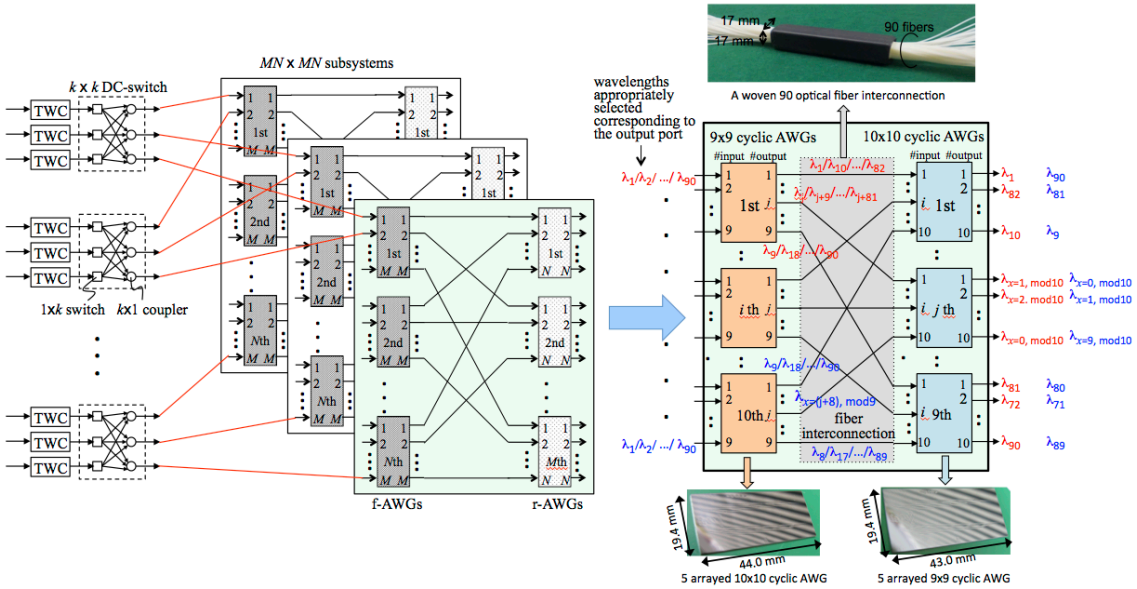

(a) *KMN* x *KMN* WP-switch architecture (K=3) (b) 90 x 90 AWG subsystem using 9 x 9 and 10 x 10 AWGs

Fig. 3 *KMN* x *KMN* WP-switch architecture (K=3) and fabricated 90 x 90 AWG subsystem

Fig. 3(a) shows the *KMN* x *KMN* WR-switch architecture with *MN* K*x*K DC-switches and *K* *MN*x*MN* AWG subsystems. The DC-switches connect each tunable laser (TL) to one of the desired AWG subsystems. These DC-switches are simple and easy to fabricate because they consist of couplers and switches that can be easily implemented with planar lightwave circuit (PLC) technology. Recently, an 8 x 12 DC-switch was fabricated on a single PLC chip and the transmission loss was reported to less than 14.5dB, including intrinsic optical coupler loss of 10.8 dB [15]. Each AWG subsystem can be realized by utilizing a single *NM* x *NM* AWG, however, the port count number is limited as mentioned before. The AWG subsystem architecture solves this problem by combining small-size cyclic AWGs as explained above (Fig. 3(a)).

PROTOTYPE SYSTEM

Fig. 3(b) shows a fabricated 90 x 90 AWG subsystem architecture consisting of ten 9 x 9 cyclic AWG and nine 10 x 10 cyclic AWG. In this example, we assume that the *i*th 9 x 9 AWG is connected to the *j*th 10 x 10 AWG so that (#output of ith 9 x 9 AWG) = *j*, and (#input of jth 10 x 10 AWG) = *i*, as one connection example (see Fig. 3(b)). *K* = 10 and 90 x 90 AWG subsystems, for example, yields a 900 x 900 large-scale optical switch. The system provides good modular growth capability in terms of each AWG.

The fabricated 9x9 cyclic AWG and 10x10 cyclic AWG have channel spacing of 50 GHz, and FSR values of 450 GHz and 500 GHz, respectively. Five 9x9 AWGs or five 10x10 AWGs are included in a single PLC chip as shown in the insertions of Fig. 3(b). A photo of the woven 90 optical fiber interconnection part between the 9 x 9 and 10 x 10 AWGs is also shown in Fig. 3(b), which is made very compactly and cost-effectively. The typical insertion loss variations on the 50 GHz spaced ITU-T grid for both AWG types are depicted in Fig. 4, where the vertical bar on each input port represents loss variations among the 90 channels. In Fig. 4 (a) and (b), the worst loss was 6.4 dB and 6.9 dB, respectively. Loss suppression in a cascade, f-AWG to r-AWG, can be achieved by changing the connecting fiber configurations between front and rear AWGs so that 9x9 and 10x10 cyclic AWGs will not exhibit large loss simultaneously as explained before. The worst loss recorded from the 90x90 subsystem was 10.2 dB, which is 3.1 dB smaller than the possible worst loss of 6.4+6.9 dB.

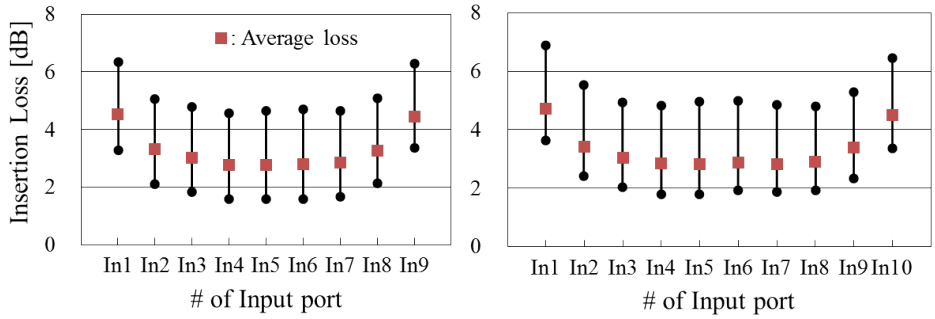

(a) 9x9 cyclic AWG (b) 10x10 cyclic AWG

Fig. 4 Typical insertion loss of cyclic AWG

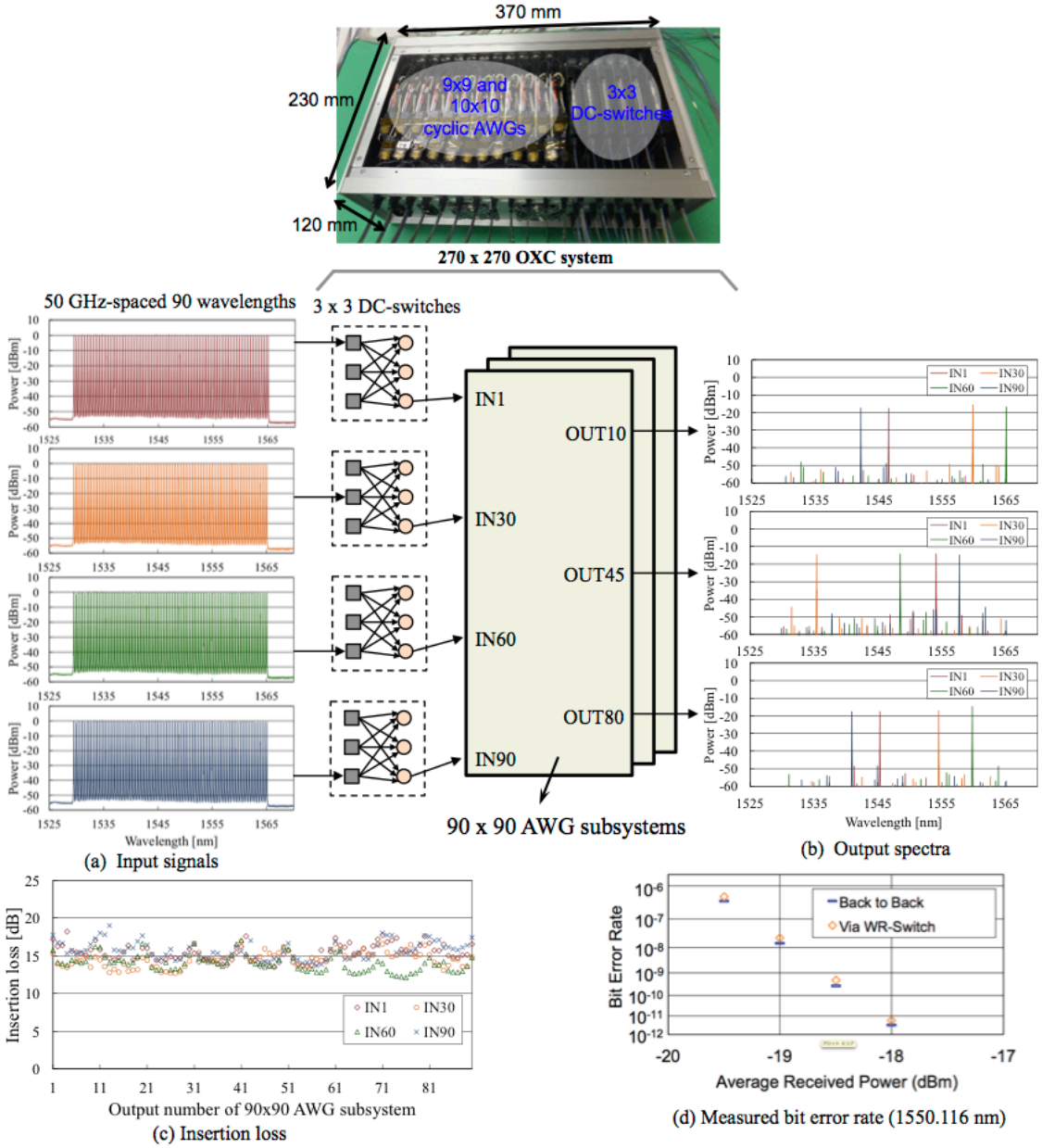

Fig. 5 Experiment on developed 270 x 270 OXC system

A 270 x 270 WR-switch was developed using ninety 3 x 3 DC-switches and three 90 x 90 AWG subsystems. Five 3 x 3 DC-switches are integrated on a small PLC chips. The average loss of the typical 3x3 DC-switch was 7.4 dB, which includes the inherent 1x3 coupler loss of 4.8 dB. The photograph in Fig. 5 shows the developed 270 x 270 WR-switch compactly assembled in a 370 x 230 x 120 mm^3 box. In order to verify the routing function, transmission experiments were executed. In this experiment, we input 90 wavelengths with 50 GHz spacing on the ITU-T grid (191. 55 +0.05 x n [THz]; n = 0 ~ 89) to different four input ports of the WR-switch simultaneously. All signals were intentionally input to the same AWG subsystem and typical output spectra at three output ports (OUT10, OUT45, OUT80) are shown in Fig. 5 (a) and (b) (four signals are routed to each port). Each wavelength was confirmed to be properly routed. Fig. 5 (c) shows the insertion loss of the system. The average and maximum loss was 14.9 and 19.0 dB. The bit error rate at 10 Gbps was also measured at the typical wavelength of 1550.116 nm, see Fig. 5 (d). The power penalty at 10^{-9} was 0.068 dB.

CONCLUSION

This article introduced a novel, highly scalable optical switch architecture that exploits the wavelength routing capability of AWGs. The resulting switches consist of small cyclic AWGs and provide excellent modular growth capabilities. A 270x270 prototype switch was fabricated using PLC technologies and we verified its technical feasibility through transmission experiments. The transmission loss that stems from relying on passive components should be compensated; pump laser shared cost-effective EDFAs or SOAs are practical solutions. Si photonics technologies or III-V semiconductor technologies may be utilized in the future, which would reduce size dramatically. The switch port count can be expanded to exceed 1,000x1,000, i.e. port counts sufficient for data center application. The wavelength routing switch requires tunable transceivers instead of fixed wavelength transceivers, which are commonly utilized for Ethernet switches, and hence the price difference between them should be considered when we apply wavelength routing optical switches.

Another potential application area of this large-scale optical switch is the reconfigurable add/drop multiplexer (ROADM). ROADMs are now widely deployed, but current ROADMs do not offer the colorless, directionless, and contentionless (CDC) add/drop capabilities that would allow flexibly bridging of any wavelength path in any transmission-line side fiber to any transponder. To allow the dynamic wavelength services envisaged and to avoid the costly manual operation of current ROADMs, CDC capabilities are of prime importance. To effectively realize these capabilities, large-scale optical switches are effective. The technologies described herein can be applied to create them.

ACKNOWLEDGEMENT

The authors would like to thank Dr. Yoshiteru Jinnouchi, NTT Electronics Co., for his contributions to the prototype system development, and Mr. Akito Nishimura, Fujikura Ltd., for his contributions in realizing the fiber interconnects. A part of this work was supported by NEDO Green IT Project and KAKENHI (23246072).

REFERENCES

[1] Cisco Global Cloud Index: Forecast and Methodology, 2011–2016.
[2] N. Farrington, “Facebook’s Data Center Network Architecture,” IEEE Optical Interconnects Conference, TuB5, Santa Fe, New Mexico, May 5-7, 2013.
[3] Cedric F. Lam, “Optoelectronic Technologies for Datacenter Networking,” OFC/NFOEC 2010, NWA3, March 2010.
[4] N. Farrington, G. Porter, S. Radhakrishnan, H. H. Bazzaz, V. Subramanya, Y. Fainman, G. Papen, A. Vahdat, “Helios: a hybrid electrical/optical switch architecture for modular data centers,” Prc. ACM SIGCOMM 2010, pp. 339-350.
[5] G. Wang, D. G. Andersen, M. Kaminsky, K. Papagiannaki, T. S. Eugene Ng, M. A. Kozuch, M. Ryan, “c-Through: Part-time Optics in Data Centers,” Proc. ACM SIGCOMM, (New Delhi, India), Aug. 2010, pp. 327-338.
[6] N. Farrington, A. Forencich, P.-C. Sun, S. Fainman, J. Ford, A. Vahdat, G. Porter, and G. Papen, “A 10 μs Hybrid Optical-Circuit/Electrical-Packet Network for Datacenters,” OFC/NFOEC 2013, Anaheim March 2013.
[7] Yong-Kee Yeo, “Large Port-Count Optical Cross-connects for Data Centers” Photonics in

Switching, Fr-S37-I12, Corsica, France, September 11-14 2012.
[8] P. N. Ji, D. Qian, K. Kanonakis, C. Kachris and I. Tomkos, "Design and Evaluation of a Flexible-Bandwidth OFDM-Based Intra Data Center Interconnect," IEEE J. of Selected Topics In Quantum Electronics, vol. 19, No. 2, March/April, 2013.
[9] A. Wonfor, H. Wang, R. V. Penty, and I. H. White, "Large Port Count High-Speed Optical Switch Fabric for Use Within Datacenters," Journal of Optical Communications and Networking, Vol. 3, Issue 8, pp. A32-A39 (2011).
[10] A. Vahdat, "Delivering scale out data center networking with optics –Why and how," OFC/NFOEC 2012, OTu1B.1, San Diego, March 2012.
[11] S. Kamei, M. Ishii, A. Kaneko, T. Shibata, and M. Itoh, "NxN Cyclic-Frequency Router With Improved Performance Based on Arrayed-Waveguide Grating," J. Lightw. Technol., vol. 27, no. 18, pp. 4097–4104, Sep. 2009.
[12] K. Sato, Advances in Transport Network Technologies: Photonic networks, ATM, and SDH, Artech House, Norwood, 1996.
[13] T. Niwa et al., "Large Port Count Wavelength Routing Optical Switch that Consists of Cascaded Small-Size Cyclic Arrayed Waveguide Gratings," IEEE Photon. Technol. Lett., vol. 24, No. 22, November 2012, pp. 2027-2030.
[14] T. Niwa, H. Hasegawa, and K. Sato, "A 270 x 270 optical cross-connect switch utilizing wavelength routing with cascaded AWGs," OFC/NFOEC 2013, OTh1A.3, Anaheim, March 17-21, 2013.
[15] T. Watanabe et al., "Silica-Based PLC Transponder Aggregators for Colorless, Directionless, and Contentionless ROADM," OFC/NFOEC 2012, OTh3D.1.

Figure Captions

Fig. 1 Wavelength routing of a cyclic AWG for different input ports
Fig. 2 Novel wavelength routing switch architecture (*MN*x*MN* subsystem) and the wavelength map (M = 4 and N = 3)
Fig. 3 *KMN* x *KMN* WP-switch architecture (K=3) and fabricated 90 x 90 AWG subsystem
(a) *KMN* x *KMN* WP-switch architecture (K=3)
(b) 90 x 90 AWG subsystem using 9 x 9 and 10 x 10AWGs
Fig. 4 Typical insertion loss of cyclic AWG
(a) 9x9 cyclic AWG, (b) 10x10 cyclic AWG
Fig. 5 Experiment on developed 270 x 270 OXC system
(a) Input signals
(b) Output spectra
(c) Insertion loss
(d) Measured bit error rate (1550.116 nm)

Table Captions

Table 1 Examples of switch scale

BIOGRAPHIES

KEN-ICHI SATO [F] is currently a professor at the graduate school of Engineering, Nagoya University, and he is an NTT R&D Fellow. Before joining the university in April 2004, he was an executive manager of the Photonic Transport Network Laboratory at NTT. His R&D activities cover future transport network architectures, network design, OA&M (operation administration and maintenance) systems, photonic network systems including optical cross-connect/ROADM and photonic IP routers, and optical transmission technologies. He has authored/co-authored more than 350 research publications in international journals and conferences. He holds 50 granted patents and more than 100 pending patents. He received his B.S., M.S., and Ph.D. degrees in electronics engineering from the University of Tokyo, Tokyo, Japan, in 1976, 1978, and 1986, respectively. He received the Young Engineer Award in 1984, the Excellent Paper Award in 1991, the Achievement Award in 2000, and the Distinguished Achievement and Contributions Award in 2012 from the Institute of Electronics, Information and Communication Engineers (IEICE) of JAPAN, and the Best Paper Awards in 2007 and 2008 from IEICE Communications Society. He was also the recipient of the distinguished achievement Award of the Ministry of Education, Science and Culture in 2002. His contributions to ATM (Asynchronous Transfer Mode) and optical network technology development extend to co-editing five IEEE JSAC special issues and the IEEE JLT special issue once, organizing several Workshops and Conference technical sessions, serving on numerous committees of international conferences including OFC and ECOC, authoring a book, Advances in Transport Network Technologies (Artech House), and co-authoring fourteen other books. He is a Fellow of the IEICE of JAPAN and a Fellow of the IEEE.

HIROSHI HASEGAWA [M] received the B.E., M.E., and D.E. degrees all in Electrical and Electronic Engineering from Tokyo Institute of Technology, Tokyo, Japan, in 1995, 1997, and 2000, respectively. From 2000 to 2005, he was an assistant professor of the Department of Communications and Integrated Systems, Tokyo Institute of Technology. Currently he is an associate professor of Nagoya University. His current research interests include Photonic Networks, Image Processing (especially Super-resolution), Multidimensional Digital Signal Processing and Time-Frequency Analysis. He received the Young Researcher Awards from SITA (Society of Information Theory and its Applications) and IEICE (Institute of Electronics, Information and Communication Engineers) in 2003 and 2005, respectively.

TOSHIO WATANABE [M]
Will come soon.

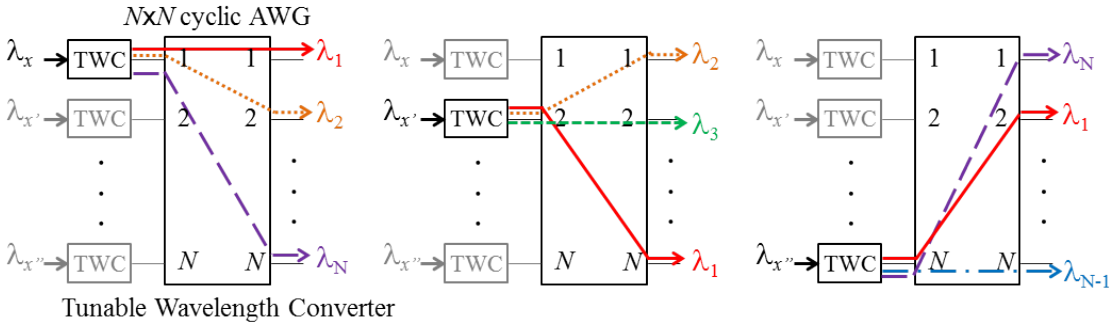

Fig. 1. Wavelength routing of a cyclic AWG for different input ports

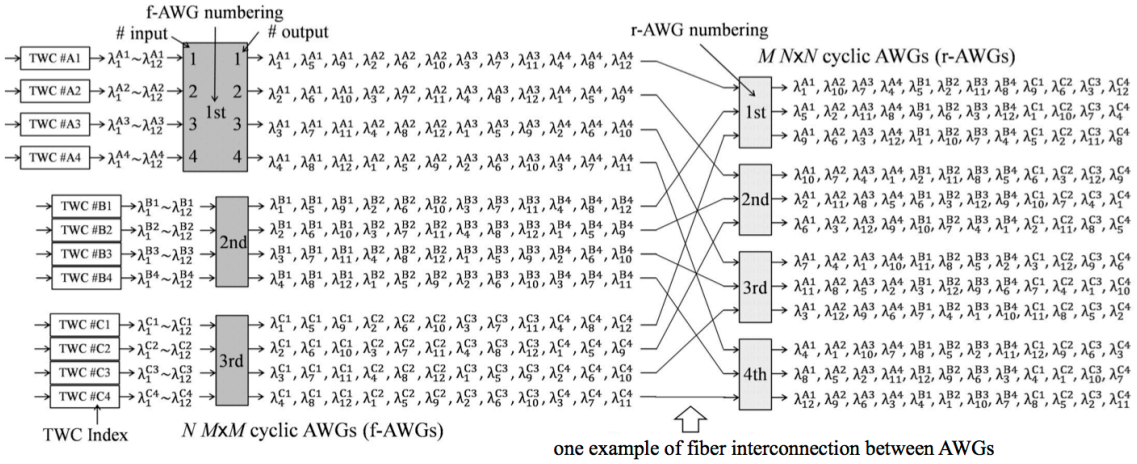

Fig. 2 Novel wavelength routing switch architecture (MNxMN subsystem) and the wavelength map (M = 4 and N = 3)

Table 1 Examples of switch scale

switch size in Fig. 2	M	N	# of necessary wavelenths
210x210	14	15	210
208x208	13	16	208
195x195	13	15	195
182x182	13	14	182
156x156	12	13	156
154x154	11	14	154
143x143	11	13	143
132x132	11	12	132
130x130	10	13	130
110x110	10	11	110
99x99	9	11	99
90x90	9	10	90
88x88	8	11	88
72x72	8	9	72
70x70	7	10	70

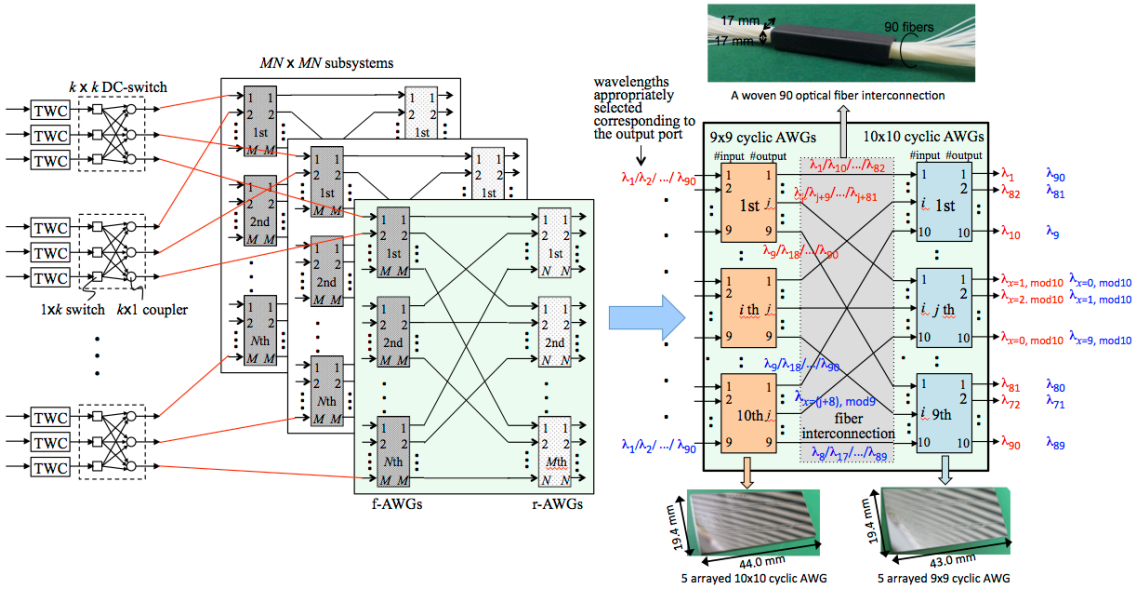

(a) *KMN* x *KMN* WP-switch architecture (K=3) (b) 90 x 90 AWG subsystem using 9 x 9 and 10 x 10 AWGs

Fig. 3 *KMN* x *KMN* WP-switch architecture (K=3) and fabricated 90 x 90 AWG subsystem

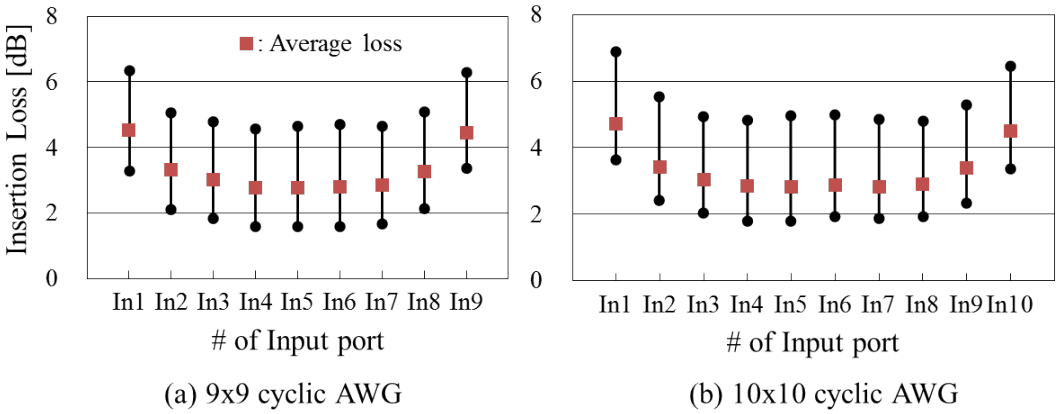

(a) 9x9 cyclic AWG (b) 10x10 cyclic AWG

Fig. 4 Typical insertion loss of cyclic AWG

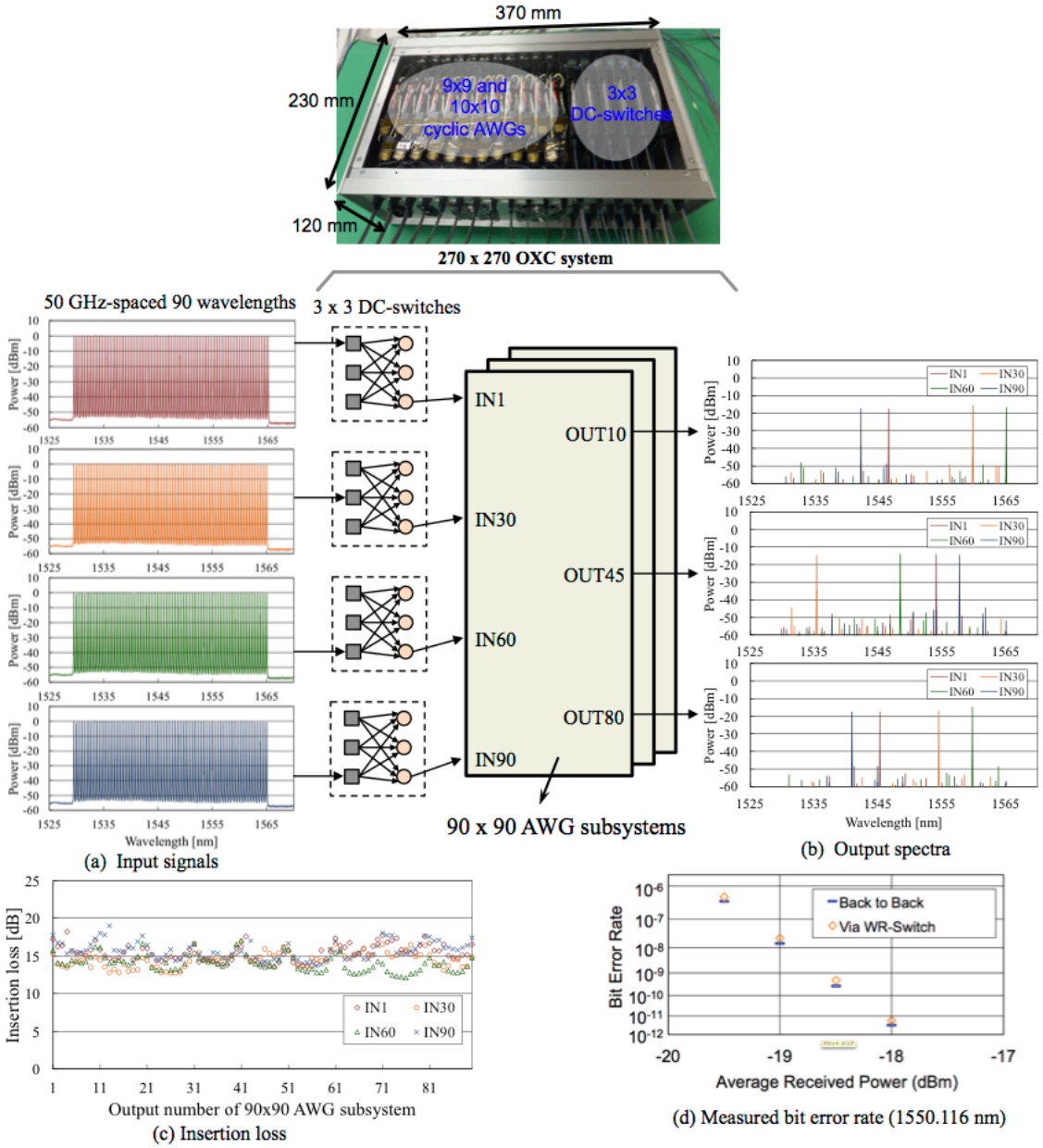

Fig. 5 Experiment on developed 270 x 270 OXC system